Proceedings of the 12th World Congress on Electrical Engineering and Computer Systems and Sciences (EECSS 2026)
August 16 – 18, 2026 – London, United Kingdom
Paper No. ICBES 154
DOI: 10.11159/icbes26.154

Comparative Evaluation of the KRAS G12D Inhibitors MRTX1133 and Zoldonrasib Using Real-Time Live-Cell Imaging

Jonathan Huang[1], Prisha Malhotra[1], Isabella Fahy[1], Ryan Lay, Shenggang Yan, Phu Nguyen, Linda Shi, Veronica Gomez-Godinez
Institute of Engineering in Medicine, University of California San Diego
9500 Gilman Drive, La Jolla, CA 92093, USA
jhsd1226@gmail.com; malhotra.prisha@gmail.com; izzyfahy8@gmail.com; rhlay@ucsd.edu; s7yan@ucsd.edu; p8nguyen@ucsd.edu; zshi@ucsd.edu; vgomez-godinez@ucsd.edu
[1]High school students participating in the IEM OPALS program

Abstract **-** Mutations in the KRAS gene, particularly the KRAS G12D variant, are among the most common oncogenic drivers in pancreatic cancer and represent an important target for precision therapy. Recent advances have led to the development of selective KRAS G12D inhibitors; however, quantitative comparison of their biological activities remains limited. In this study, we compared the cytotoxic effects of two KRAS G12D inhibitors, MRTX1133 and Zoldonrasib, using the Agilent xCELLigence RTCA eSight live-cell imaging platform. AsPC-1 pancreatic cancer cells were treated with MRTX1133 (10 pM, 1 nM, and 100 nM) or Zoldonrasib (1 nM, 10 nM, and 100 nM), and drug-induced cell death was continuously monitored for 120 hours using DeadRed fluorescence imaging. Both compounds demonstrated concentration-dependent cytotoxic responses. MRTX1133 produced a gradual increase in normalized dead-cell percentage, reaching approximately 15% at 100 nM after 120 hours. In comparison, Zoldonrasib induced a substantially stronger response, with approximately 30% normalized dead cells at the same concentration. Student's *t*-test analysis confirmed statistically significant increases in cell death for the 100 nM treatment groups compared with the DMSO control, whereas lower concentrations produced weaker or nonsignificant responses. Direct comparison of the two inhibitors demonstrated that Zoldonrasib consistently exhibited greater cytotoxic activity than MRTX1133 under identical experimental conditions. These findings demonstrate the value of real-time live-cell imaging for quantitative evaluation of targeted anticancer therapies and suggest that Zoldonrasib may exhibit greater in vitro cytotoxic efficacy than MRTX1133 against KRAS G12D-mutant pancreatic cancer cells.

Keywords**:** KRAS G12D; MRTX1133; Zoldonrasib; pancreatic cancer; AsPC-1; targeted therapy; live-cell imaging; RTCA eSight; cytotoxicity

1. Introduction

Pancreatic ductal adenocarcinoma (PDAC) remains one of the deadliest human malignancies, with a five-year survival rate of approximately 13% despite advances in diagnosis and treatment [1]–[3]. The poor prognosis is largely attributed to late-stage diagnosis, rapid disease progression, and the limited effectiveness of conventional chemotherapy. Among the molecular alterations identified in PDAC, activating mutations in the KRAS oncogene are present in more than 90% of cases, with the KRAS G12D mutation representing the most common variant [4], [5]. Constitutive activation of KRAS drives persistent signaling through the RAF–MEK–ERK and PI3K–AKT pathways, promoting uncontrolled proliferation, resistance to apoptosis, metabolic reprogramming, and tumor progression [5], [6].

For many years, KRAS was considered an "undruggable" target because of its high affinity for GTP and the absence of suitable binding pockets for small-molecule inhibitors [6]. Recent advances in structural biology, medicinal chemistry, and protein degradation technologies have transformed this landscape, leading to the development of mutation-selective KRAS inhibitors and degraders [5]–[7]. While inhibitors targeting the KRAS G12C mutation have already entered clinical practice, selective therapies against KRAS G12D have emerged only recently and represent an important new direction for precision oncology [5], [7].

Among these next-generation therapeutics, MRTX1133 is a highly selective, noncovalent inhibitor that binds specifically to KRAS G12D and has demonstrated potent antitumor activity in preclinical studies [5]. Zoldonrasib is another promising KRAS G12D-targeted inhibitor currently undergoing preclinical and early clinical evaluation. As additional

KRAS G12D inhibitors become available, direct comparisons of their biological activity using standardized experimental platforms will become increasingly important for understanding differences in efficacy and guiding future therapeutic development.

Although conventional chemotherapeutic agents remain the standard of care for many patients with pancreatic cancer, they are frequently associated with significant toxicity and drug resistance [8]–[10]. In contrast, targeted therapies aim to selectively inhibit oncogenic signaling while minimizing damage to normal tissues. However, targeted inhibitors may produce either cytotoxic effects, characterized by cancer cell death, or cytostatic effects, characterized primarily by suppression of cellular proliferation [11], [12]. Distinguishing between these biological responses is therefore essential for accurately evaluating therapeutic efficacy.

In this study, we employed the Agilent xCELLigence RTCA eSight live-cell imaging platform to compare the responses of AsPC-1 pancreatic cancer cells to MRTX1133 and Zoldonrasib. Continuous fluorescence imaging was used to quantify treatment-induced cell death by monitoring the normalized DeadRed fluorescence signal over a 120-hour period. By integrating real-time imaging with quantitative statistical analysis, this study provides a comparative evaluation of two emerging KRAS G12D inhibitors and demonstrates the utility of multi-parameter live-cell imaging for assessing targeted anticancer therapies.

2. Materials and Method

2.1. Cell Culture and Drug Treatment

Human pancreatic adenocarcinoma AsPC-1 cells were cultured under standard cell culture conditions in a humidified incubator at 37°C with 5% CO_2. Cells were seeded into Agilent RTCA eSight E-Plate VIEW 96-well plates and allowed to attach prior to drug treatment.

Two KRAS G12D inhibitors, MRTX1133 and Zoldonrasib, were evaluated independently. MRTX1133 was tested at 10 pM, 1 nM, and 100 nM, whereas Zoldonrasib was tested at 1 nM, 10 nM, and 100 nM. These concentration ranges were selected based on the reported in vitro activity of each compound and preliminary optimization studies. Cells treated with 0.1% DMSO served as the vehicle control

2.2. Real-Time Live-Cell Imaging

Following drug treatment, cell responses were continuously monitored for 120 hours using the Agilent xCELLigence RTCA eSight Live-Cell Analysis System. Brightfield and fluorescence images were automatically acquired at predetermined time intervals throughout the experiment.

Dead cells were labeled using the DeadRed™ fluorescent reagent, while cell nuclei were stained with DAPI. The RTCA eSight platform enabled simultaneous visualization of cellular morphology and fluorescence signals, allowing continuous assessment of drug-induced cytotoxicity without disturbing the cultures.

2.3. Image Processing and Quantitative Analysis

Fluorescence images were analyzed using the Agilent RTCA eSight image analysis software. DeadRed-positive cells were quantified to determine the percentage of dead cells at each imaging time point. The resulting values were normalized to the initial measurement to facilitate comparison among treatment groups.

Representative fluorescence images were used to illustrate cellular morphology and staining patterns, while quantitative time-course plots were generated to compare cytotoxic responses among the different treatment conditions.

To directly compare the efficacy of the two KRAS G12D inhibitors, the 100 nM treatment groups for MRTX1133 and Zoldonrasib were analyzed together. This comparison enabled evaluation of their relative cytotoxic effects under identical experimental conditions.

2.4. Statistical Analysis

Data are presented as mean ± standardized Error Mean (SEM). Statistical analyses were performed using google sheet. Differences between each treatment group and the DMSO control were evaluated using unpaired two-tailed Student's *t*-tests at each time point.

Statistical significance was defined as $p < 0.05$. Significance levels are indicated as $p < 0.05$ (*), $p < 0.01$ (**), $p < 0.001$ (***), and $p < 0.0001$ (****). The statistical results are summarized in Table 1.

3. Results and Discussion

3.1. Cytotoxic Effects of MRTX1133 and Zoldonrasib

To compare the cytotoxic effects of two KRAS G12D inhibitors, MRTX1133 and Zoldonrasib, AsPC-1 pancreatic cancer cells were continuously monitored for 120 hours using the Agilent xCELLigence RTCA eSight live-cell imaging platform. Drug-induced cytotoxicity was quantified by measuring the normalized DeadRed fluorescence signal over time.

As shown in Figure 1, MRTX1133 produced a concentration-dependent increase in cancer cell death. The DMSO control remained below approximately 3% normalized dead cells throughout the experiment. Treatment with 10 pM resulted in minimal changes compared with the control, whereas 1 nM produced a moderate increase in DeadRed fluorescence during the later stages of the experiment. The strongest cytotoxic response was observed with 100 nM MRTX1133, where the normalized dead-cell percentage gradually increased to approximately 15% after 120 hours. These findings demonstrate that MRTX1133 induces measurable cytotoxicity in AsPC-1 cells, with increasing activity observed at higher drug concentrations.

Figure 2 illustrates the response of AsPC-1 cells treated with Zoldonrasib. Similar to MRTX1133, Zoldonrasib exhibited a concentration-dependent increase in cytotoxicity. Treatment with 1 nM produced only a slight increase in dead-cell percentage, while 10 nM generated a moderate response. In contrast, 100 nM Zoldonrasib produced a continuous increase in DeadRed fluorescence throughout the experiment, reaching approximately 30% normalized dead cells after 120 hours. This response was substantially greater than that observed with MRTX1133, indicating stronger induction of cancer cell death under the experimental conditions evaluated.

3.2. Direct Comparison Between MRTX1133 and Zoldonrasib

To directly compare the cytotoxic activities of the two KRAS G12D inhibitors, the 100 nM treatment groups were plotted together in Figure 3. Both compounds produced progressive increases in the normalized dead-cell percentage relative to the DMSO control. However, Zoldonrasib consistently generated higher DeadRed fluorescence than MRTX1133 throughout the experiment. The difference between the two treatment groups became apparent during the early phase of drug exposure and continued to increase over time. By the end of the 120-hour monitoring period, 100 nM Zoldonrasib produced approximately 30% normalized dead cells, whereas 100 nM MRTX1133 reached approximately 15%, representing nearly a two-fold difference in cytotoxic response. These results suggest that Zoldonrasib exhibits greater in vitro cytotoxic activity than MRTX1133 against KRAS G12D-mutant AsPC-1 pancreatic cancer cells.

3.3. Statistical Analysis

Student's *t*-tests were performed to compare each treatment group with the DMSO control at individual time points (Table 1). For MRTX1133, statistically significant increases in dead-cell percentage were primarily observed in the 100 nM treatment group, whereas the 10 pM and 1 nM groups showed only limited or no significant differences from the control during most of the experiment. For Zoldonrasib, the 100 nM treatment group also demonstrated highly significant increases in dead-cell percentage throughout the latter portion of the experiment, while the 1 nM and 10 nM treatment groups exhibited comparatively weaker responses.

Overall, both KRAS G12D inhibitors demonstrated concentration-dependent cytotoxicity in AsPC-1 cells. However, Zoldonrasib consistently produced a greater magnitude of cell death than MRTX1133 at the shared concentration of 100 nM, suggesting stronger antitumor activity under identical experimental conditions. These findings further demonstrate the utility of the Agilent xCELLigence RTCA eSight platform for quantitatively comparing the biological responses of targeted anticancer therapies in real time.

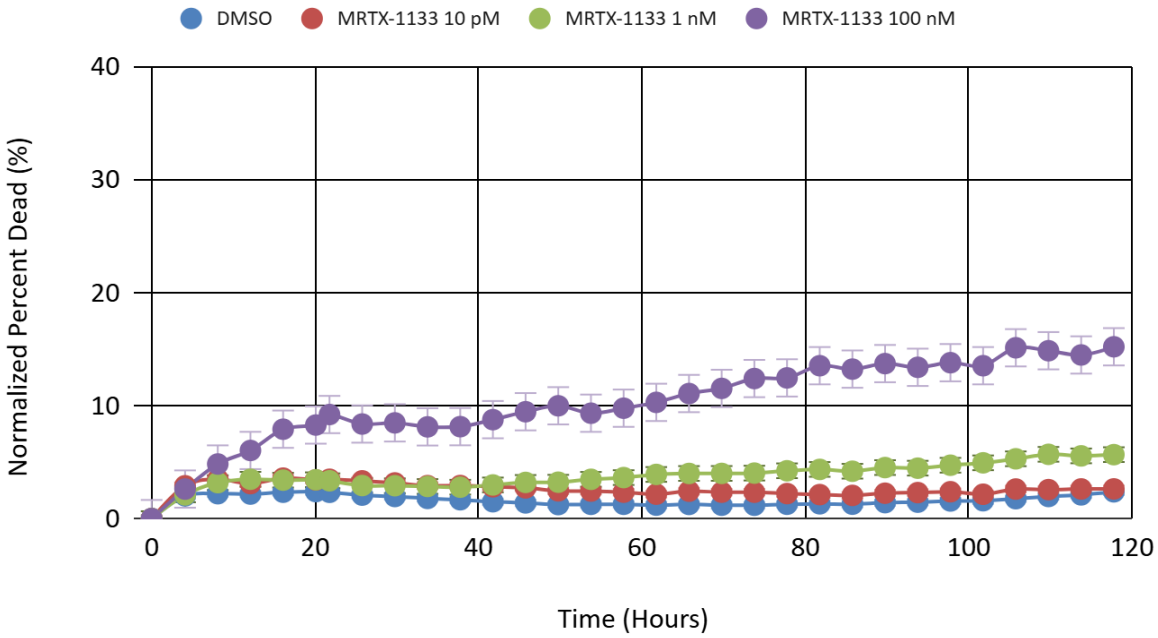

Fig. 1: Time-dependent changes in normalized dead-cell percentage of AsPC-1 pancreatic cancer cells treated with MRTX1133 (10 pM, 1 nM, and 100 nM). Dead-cell accumulation was continuously monitored for 120 hours using the Agilent xCELLigence RTCA eSight system. The DMSO-treated group served as the vehicle control.

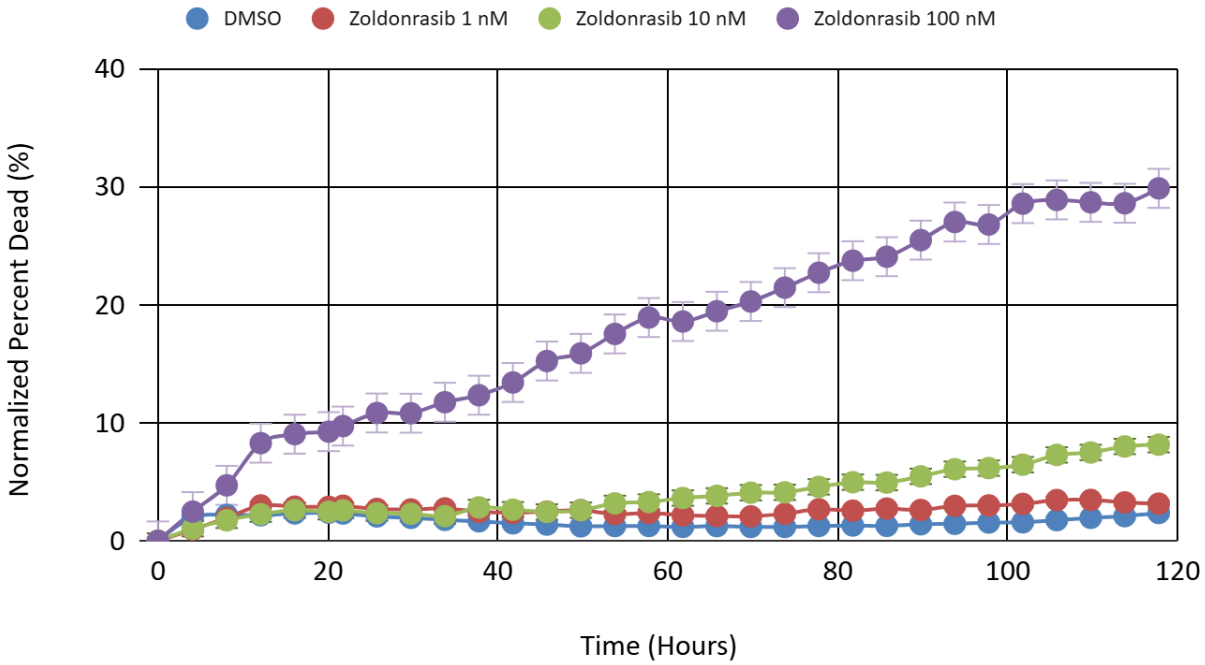

Fig. 2: Time-dependent changes in normalized dead-cell percentage of AsPC-1 pancreatic cancer cells treated with Zoldonrasib (1 nM, 10 nM, and 100 nM). Dead-cell accumulation was continuously monitored for 120 hours using the Agilent xCELLigence RTCA eSight system. The DMSO-treated group served as the vehicle control.

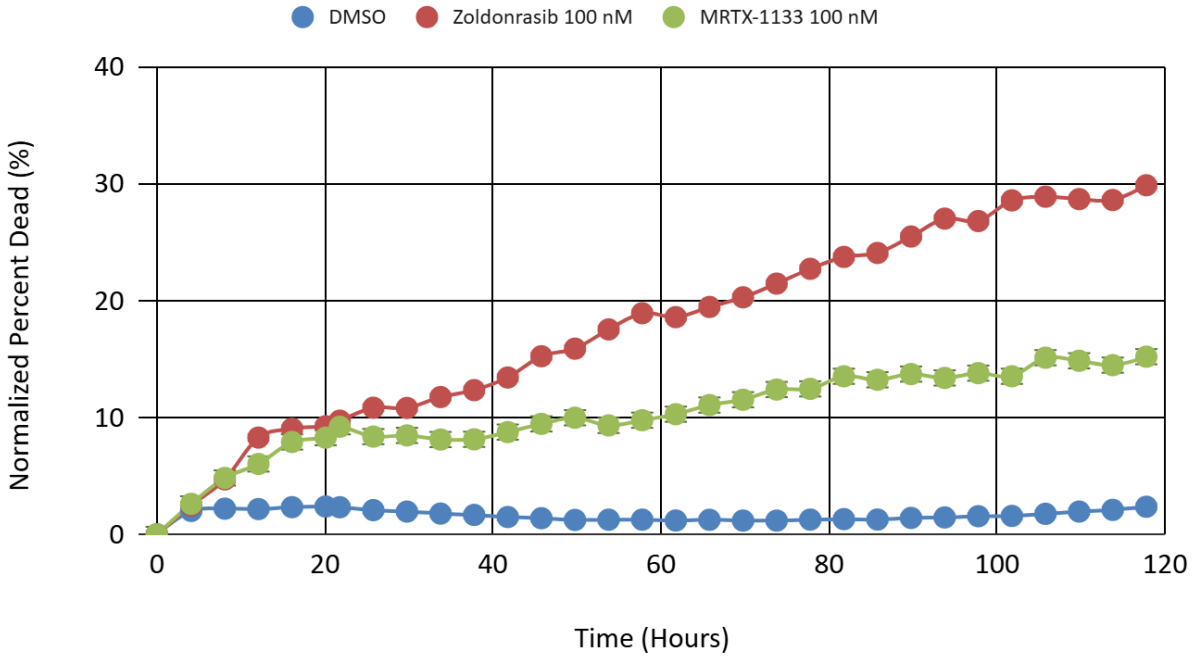

Fig. 3 Direct comparison of normalized dead-cell percentage between 100 nM MRTX1133 and 100 nM Zoldonrasib in AsPC-1 pancreatic cancer cells over 120 hours. Zoldonrasib produced consistently greater cytotoxicity than MRTX1133 throughout the monitoring period.

Table 1 Statistical Comparison of Drug-Treated Groups with the DMSO Control Using Student's *t*-test

Time (Hours)	Zoldonrasib 1 nM	Zoldonrasib 10 nM	Zoldonrasib 100 nM	MRTX-1133 10 pM	MRTX-1133 1 nM	MRTX-1133 100 nM
4	0.06490	0.12986	0.42200	0.19040	0.89360	0.33478
8	0.66757	0.50699	0.00121	0.07350	0.21137	0.00019
12	0.17089	0.89647	0.00001	0.12345	0.06987	0.00002
16	0.43162	0.74493	0.00000	0.05292	0.12330	0.00000
20	0.60539	0.93865	0.00000	0.23082	0.26645	0.00001
22	0.49134	0.80271	0.00000	0.16312	0.23299	0.00000
26	0.43270	0.76735	0.00000	0.05943	0.23641	0.00000
30	0.32820	0.71055	0.00000	0.06402	0.13662	0.00000
34	0.15531	0.73105	0.00000	0.05576	0.09882	0.00000
38	0.17775	0.18785	0.00000	0.02240	0.05168	0.00000
42	0.14468	0.28562	0.00000	0.01789	0.01841	0.00000

46	0.05447	0.29608	0.00000	0.01066	0.00191	0.00000	
50	0.00850	0.20008	0.00000	0.00990	0.00052	0.00000	
54	0.03663	0.06273	0.00000	0.01643	0.00012	0.00000	
58	0.02174	0.06907	0.00000	0.03128	0.00013	0.00000	
62	0.05372	0.02885	0.00000	0.05021	0.00002	0.00000	
66	0.08204	0.02519	0.00000	0.02418	0.00001	0.00000	
70	0.06914	0.02042	0.00000	0.02126	0.00000	0.00000	
74	0.02333	0.01538	0.00000	0.01692	0.00000	0.00000	
78	0.00469	0.00842	0.00000	0.04915	0.00000	0.00000	
82	0.01208	0.00329	0.00000	0.09134	0.00000	0.00000	
86	0.00377	0.00236	0.00000	0.09085	0.00000	0.00000	
90	0.00647	0.00073	0.00000	0.05185	0.00000	0.00000	
94	0.00139	0.00033	0.00000	0.05720	0.00000	0.00000	**P > 0.05**
98	0.00368	0.00090	0.00000	0.10876	0.00000	0.00000	*** P < 0.05**
102	0.00359	0.00091	0.00000	0.27091	0.00000	0.00000	**** P < 0.01**
106	0.00261	0.00017	0.00000	0.13204	0.00000	0.00000	***** P < 0.005**
110	0.01103	0.00025	0.00000	0.30915	0.00000	0.00000	****** P < 0.001**
114	0.04907	0.00003	0.00000	0.37151	0.00000	0.00000	
118	0.15182	0.00010	0.00000	0.65011	0.00000	0.00000	
Average	0.14234	0.24791	0.01411	0.11391	0.07807	0.01117	
	ns	ns	* s	ns	ns	* s	

4. Conclusion

This study demonstrates that ZA001222 (MRTX1133), a selective noncovalent KRAS G12D inhibitor, produces a measurable and consistent inhibitory effect on the proliferation of AsPC-1 pancreatic cancer cells, characterized by moderate-to-strong cytostatic suppression of growth with limited cytotoxicity. Real-time kinetic monitoring using the xCELLigence RTCA eSight system enabled dynamic, multi-parameter assessment of drug response across a 48-hour experimental window.

Brightfield confluence tracking confirmed a dose-dependent reduction in cell proliferation, with treated groups reaching a growth plateau at approximately 30 hours and exhibiting a 45–55% reduction in normalized confluence at 48 hours compared to untreated controls. Dead-cell staining (DeadRed channel) revealed no statistically significant increase in cytotoxicity across any tested concentration, establishing that the observed growth suppression is attributable to cytostatic arrest rather than direct cell lysis. Live-cell quantification via the blue channel corroborated these findings, with a 30–45% reduction in DAPI-positive nuclear counts in treated groups relative to controls.

These results support the further development of MRTX1133 as a targeted therapeutic for KRAS G12D-driven cancers and validate the xCELLigence RTCA eSight platform as a practical and sensitive tool for evaluating targeted inhibitors in vitro. Importantly, variability in response magnitude across experimental conditions highlights the need for continued profiling across a broader panel of cancer cell lines and co-mutation contexts to fully delineate the spectrum of KRAS G12D-targeted therapy responsiveness.

Future studies should incorporate extended time-course experiments, patient-derived cell models, and combination treatment regimens to clarify response variability and evaluate potential synergies with existing standard-of-care therapies. Pathway-specific assays targeting KRAS downstream effectors, including ERK phosphorylation and AKT activation, will further elucidate the molecular basis of drug sensitivity and resistance in KRAS G12D-mutant tumors.

Acknowledgements

This study was conducted with a gift from Beckman Laser Institute Inc. to LS and VGG. We gratefully acknowledge the support of Leighton Foundation, Ming-Wei Wu, Shu Chien, Lizhu Chen (CorDx Inc.), Xinhua Zheng, David and Leslie Lee, and Mingwei He and Wen Shi.

References

[1] C. Sesock, "Pancreatic cancer deaths continue to rise; five-year survival rate remains stalled at 13% while all cancers combined reach milestone 70%," Pancreatic Cancer Action Network, Jan. 13, 2026. https://pancan.org/press-releases/pancreatic-cancer-deaths-continue-to-rise-five-year-survival-rate-remains-stalled-at-13-while-all-cancers-combined-reach-milestone-70/

[2] Pancreatic Cancer Action Network, "Pancreatic cancer facts 2016," 2016. [Online]. Available: https://pancan.org/wp-content/uploads/2016/02/2016-GAA-PC-Facts.pdf. [Accessed: Jun. 6, 2026].

[3] National Cancer Institute, "Cancer of the pancreas - cancer stat facts," SEER, 2024. [Online]. Available: https://seer.cancer.gov/statfacts/html/pancreas.html

[4] A. Brink, "Opinion: KRAS mutations provide prognostic insights and expand treatment options," Oncology Nursing News, Feb. 21, 2024. [Online]. Available: https://www.oncnursingnews.com/view/opinion-kras-mutations-provide-prognostic-insights-and-expand-treatment-options

[5] M. N. Zeissig, L. M. Ashwood, O. Kondrashova, and K. D. Sutherland, "Next batter up! Targeting cancers with KRAS-G12D mutations," Trends in Cancer, vol. 9, no. 11, 2023, doi: 10.1016/j.trecan.2023.07.010.

[6] L. Huang, Z. Guo, F. Wang, and L. Fu, "KRAS mutation: From undruggable to druggable in cancer," Signal Transduction and Targeted Therapy, vol. 6, no. 1, Art. no. 386, Nov. 2021, doi: 10.1038/s41392-021-00780-4.

[7] T. Yoshinari, T. Nagashima, H. Ishioka, K. Inamura, Y. Nishizono, M. Tasaki, K. Iguchi, A. Suzuki, C. Sato, A. Nakayama, Y. Amano, Y. Tateishi, Y. Yamanaka, F. Osaki, M. Yoshino, K. Kuramoto, T. Imaizumi, and M. Hayakawa, "Discovery of KRAS(G12D) selective degrader ASP3082," Communications Chemistry, vol. 8, no. 1, Art. no. 254, Aug. 2025, doi: 10.1038/s42004-025-01662-4.

[8] P. Jiang, K. Zong, D. Peng, B. Zhou, and Z. Wu, "Risk comparison of adverse reactions between gemcitabine monotherapy and gemcitabine combined with albumin-bound paclitaxel in pancreatic cancer: Insights from the FDA Adverse Event Reporting System (FAERS) database," BMC Pharmacology and Toxicology, vol. 26, no. 1, Mar. 2025, doi: 10.1186/s40360-025-00884-5.

[9] T. V. Bagnyukova, I. G. Serebriiskii, Y. Zhou, E. A. Hopper-Borge, E. A. Golemis, and I. Astsaturov, "Chemotherapy and signaling," Cancer Biology & Therapy, vol. 10, no. 9, pp. 839–853, Nov. 2010, doi: 10.4161/cbt.10.9.13738.

[10] M. Mollaei, Z. M. Hassan, F. Khorshidi, and L. Langroudi, "Chemotherapeutic drugs: Cell death- and resistance-related signaling pathways. Are they really as smart as the tumor cells?," Translational Oncology, vol. 14, no. 5, Art. no. 101056, May 2021, doi: 10.1016/j.tranon.2021.101056.

[11] J. V. Anttila, M. Shubin, J. Cairns, F. Borse, Q. Guo, T. Mononen, I. Vázquez-García, O. Pulkkinen, and V. Mustonen, "Contrasting the impact of cytotoxic and cytostatic drug therapies on tumour progression," PLOS Computational Biology, vol. 15, no. 11, Art. no. e1007493, Nov. 2019, doi: 10.1371/journal.pcbi.1007493.

[12] L. M. Kim, P. Y. Kim, Y. K. Gebreyohannes, and C. T. Leung, "Sustained oncogenic signaling in the cytostatic state enables targeting of nonproliferating persistent cancer cells," Cancer Research, vol. 82, no. 17, pp. 3045–3057, Jul. 2022, doi: 10.1158/0008-5472.CAN-21-2908.